Pergamon

Int. J. Heat Mass Transfer. Vol. 39, No. 18, pp. 3931–3947, 1996

0017-9310/96 $15.00+0.00

PII: S0017-9310(96)00032-4

Heat transfer by forced convection in pipes packed with porous media whose matrices are composed of spheres

M. VARAHASAMY and R. M. FAND†

Department of Mechanical Engineering, University of Hawaii at Manoa, Honolulu, HI 96822, U.S.A.

(*Received* 5 *October* 1995 *and in final form* 13 *December* 1995)

Abstract—Empirical correlation equations for the average Nusselt number have been determined that accurately represent an extensive body of new experimental data for the geometry under consideration for fully developed thermal conditions. The equations cover the Darcy, Forchheimer and turbulent regimes of flow. The correlation equations are based upon a hypothesis that regards the flow in a porous medium to be the superposition of a 'fine' component upon a 'coarse' component and takes into account the wall effect and dispersion. The results show that packed tubes provide heat transfer rates from two to seven times those of unpacked tubes for laminar flow and two to two and a half times for turbulent flow for equal pumping power. Copyright © 1996 Elsevier Science Ltd.

STATEMENT OF OBJECTIVES

Several studies relating to heat transfer by forced convection in tubes packed with spheres have been published to date, but every such study has dealt with a gaseous medium (commonly air) as the saturating fluid and no experimental data with liquids have heretofore been available. Furthermore, numerical models currently used to study heat transfer in pipes packed with spheres do not predict heat transfer coefficients accurately for potentially useful ranges of the variable D/d, where D and d represent the pipe and sphere diameters (characteristic dimensions), respectively. Thus, designers of heat transfer equipment involving porous media lack necessary information.

The preceding observation provided the motivation for undertaking the present study. The objectives of the present work were to conduct and correlate the results of experiments with a liquid (water) in the range of $1.14 \leqslant D/d \leqslant 14.93$ for laminar and turbulent flow. Also the enhancement of heat transfer achievable by packing pipes with spheres will be compared with two other common enhancement techniques, namely, the use of twisted tape inserts and integral fins.

REVIEW OF THE LITERATURE

Fluid flow in porous media

In order to deal with the problem of forced convection heat transfer from a circular tube packed internally with saturated porous media, it is first necessary to have certain information concerning the isothermal flow of fluids through porous media. Fand *et al.* [1] have studied the three recognized regimes of flow through infinite porous media whose matrices are composed of spheres, namely, the Darcy regime (where $Re_d \leqslant Re_{DH}$‡ $= 2.3$), the Forchheimer regime (where $5 = Re_{FL} \leqslant Re_d \leqslant Re_{FH} = 80$) and the turbulent regime (where $Re_d \geqslant Re_{TL} = 120$) plus the two regions of transition between these three regimes. The values of the lower and upper bounds of the flow regimes indicated above have been determined experimentally for dimension ratios $D/d \geqslant 1.4$. For $1.08 \leqslant D/d \leqslant 1.40$¶ Fand *et al.* [3] found that the upper and lower bounds of all three regimes of flow depend on the value of D/d and can be represented by the following set of linear equations:

$$Re_{DH} = 10.6\text{–}5.90(D/d) \tag{1}$$

$$Re_{FL} = 376.5\text{–}265.6(D/d) \tag{2}$$

$$Re_{FH} = 707.0\text{–}488.2(D/d) \tag{3}$$

$$Re_{TL} = 982.1\text{–}616.2(D/d). \tag{4}$$

In their study of fluid flow through porous media Fand *et al.* [1] determined that the following equations characterize the flow adequately for $D/d > 40$:

$$f' = \frac{36\kappa}{Re'_d} \text{ for Darcy flow}; (\kappa = 5.34), \tag{5}$$

† Author to whom correspondence should be addressed.

‡ The subscript DH is a mnemonic devise which refers to the highest value (H) of the particle Reynolds number for which Darcy (D) flow occurs. Similar subscripts are used to indicate the lowest value (L) of the particle Reynolds number for which a particular type of flow occurs.

¶ $D/d = 1$ represents the lower bound for this ratio, for at this value the sphere diameter and tube diameter are equal and no flow through the tube can occur.

NOMENCLATURE

A, A' first Ergun constants per equations (6) and (7)
A_w, A'_w first Ergun–Reichelt constants per equations (9) and (10)
B, B' second Ergun constants per equations (6) and (7)
B_w, B'_w second Ergun–Reichelt constants per equations (9) and (10)
c_p specific heat of a (saturating) fluid at constant pressure
D diameter of a heated tube
d diameter of a spherical particle
Di dimensionless measure of dispersion per equation (27)
f' modified friction factor, $P'd/\rho u^2\beta_\varepsilon$
f_w wall modified friction factor, f'/M
h heat transfer coefficient
I electric current flow
k thermal conductivity
k_d thermal dispersion conductivity
k_f thermal conductivity of the fluid saturating a porous medium
k_s thermal conductivity of the solid particles in a porous medium
k_λ effective thermal conductivity per equation (19)
L active (heated) length of a tube
ΔL length of a sub-section of a tube
M wall correction factor, $1+2d/3D(1-\varepsilon)$
Nu Nusselt number, hD/k
Pe Peclet number, $Re_D Pr$
Pr Prandtl number, $\mu c_p/k$
q' rate of convective heat transfer per unit length of tube
q'' rate of convective heat transfer per unit surface area of tube
$(q_l)'$ rate of external heat loss per unit length of tube
Re_D cylinder Reynolds number, uD/ν
Re_d particle Reynolds number, ud/ν
Re'_d modified particle Reynolds number, $Re_d/(1-\varepsilon)$
Re_w wall modified Reynolds number, Re'_d/M
St Stanton number, $Nu/(Re_D\, Pr)$
T_b bulk temperature of a fluid
T_0 bulk temperature of the fluid at the inlet of a tube
T_w temperature of the inner surface of a heated tube
ΔT $\Delta T = (T_w - T_b)$
u flow speed in a porous medium
X axial distance from the inlet of a tube.

Greek symbols
β_ε a function of ε, $(1-\varepsilon)/\varepsilon^3$
ε porosity
κ Kozeny–Carman factor per equation (5)
κ_w wall-corrected Kozeny–Carman factor per equation (8)
λ conductivity ratio, k_f/k_s
ρ density of a fluid
ν kinematic viscosity of a fluid.

Subscripts
bot refers to the bottom of a horizontal tube
cal refers to a calculated value
exp refers to an experimentally determined value
i refers to a quantity associated with the particular axial location i of a tube
ls refers to laminar flow in a smooth tube
top refers to the top of a horizontal tube
ts refers to turbulent flow in a smooth tube.

Error notation
E percent error: $[(Nu_{exp} - Nu_{cal})/Nu_{exp}] \times 100\%$
E_d percent deviation of error, $|E|$
E_m percent mean error, $(\Sigma_{i=1}^{N} E_i)/N$
E_{md} percent mean deviation of error, $(\Sigma_{i=1}^{N} |E_i|)/N$
E_{maxd} percent maximum deviation of error.

$$f' = \frac{A}{Re'_d} + B \text{ for Forchheimer flow;} \quad (A = 182; B = 1.92), \quad (6)$$

$$f' = \frac{A'}{Re'_d} + B' \text{ for turbulent flow;} \quad (A' = 225; B' = 1.61), \quad (7)$$

where $f' = P'd/\rho u^2\beta_\varepsilon$ is called the modified friction factor and $Re'_d = Re_d/(1-\varepsilon)$ is called the modified particle Reynolds number.

The transition regions between Darcy and Forchheimer flow and between Forchheimer and turbulent flow are difficult to characterize because they cannot be represented by simple equations such as equations (5), (6) or (7). It was shown in ref. [1] that this difficulty can be overcome without incurring significant error by assuming that fictitious transition points exist, denoted by Re_{DF} and Re_{FT}, at which the flow abruptly changes from Darcy to Forchheimer and from Forchheimer to turbulent flow. The numerical values of Re_{DF} and Re_{FT} are 3 and 100, respectively.

The effect of the wall on the flow in a porous medium

When a porous medium whose matrix is composed of discrete solid particles is confined in a duct, the wall of the duct affects the local magnitude of the porosity, ε, because the spatial distribution of the particles must conform with the shape of the wall. This is called the 'wall effect'. In order to account for the wall effect, Riechelt [4] defined the following 'wall modified' parameters: $f_w = f'/M$ and $Re_w = Re'_d/M$, where $M = 1+2d/3D(1-\varepsilon)$, with which equations (5)–(7) can be written as follows:

$$f_w Re_w = 36\,\kappa_w/M^2, \tag{8}$$

$$f_w Re_w = A_w + B_w Re_w \tag{9}$$

$$f_w Re_w = A'_w + B'_w Re_w. \tag{10}$$

The quantity κ_w is called the wall-corrected Kozeny–Carman factor. A_w, B_w and A'_w, B'_w are referred to as the first and second Ergun–Riechelt constants for Forchheimer and turbulent flow, respectively. It was shown in ref. [2] that, for $D/d \geqslant 1.4$, each of these five wall-corrected flow parameters can be represented by correlation equations having the following common form:

$$Y = Y_\infty - a[e^{-f(D/d)}], \tag{11}$$

where Y represents a wall-corrected parameter, Y_∞ represents the asymptotic value of that parameter, and $f(D/d) = p(D/d)^3 + q(D/d)^2 + r(D/d)$. The numerical values of Y_∞ and the correlation constants, (a, p, q, r) for all five flow parameters are given in ref. [2].

For the range $1.08 \leqslant D/d \leqslant 1.40$, it was shown in ref. [3] that each of the five wall-corrected flow parameters can be represented by a different correlation equation having the following common form:

$$Y = a + b(D/d) + c(D/d)^2, \tag{12}$$

where a, b and c are constants whose values are provided in ref. [3].

The following experimentally determined expressions for average porosity, ε, were presented in ref. [2]:

$$\varepsilon = 0.151/(D/d-1) + 0.360 \quad \text{for } D/d \geqslant 2.033, \tag{13}$$

$$\varepsilon = -0.6649(D/d) + 1.8578 \quad \text{for } 1.866 \leqslant D/d < 2.033, \tag{14}$$

$$\varepsilon = \left[1 - \frac{2}{3}\left(\frac{d}{D}\right)^3 \middle/ \sqrt{\frac{2d}{D} - 1}\right] \quad \text{for } 1 < D/d < 1.886. \tag{15}$$

Equations (13)–(15) together provide an algebraic representation of the maximum value of ε for all D/d. However, it should be noted that the average porosity of a tube packed with spheres can in practice depend upon several factors in addition to D/d, including the packing procedure, the surface roughness of the particles and the elasticity of the packing material. For values of $D/d < 2$ the packing is usually geometrically determinate (or very nearly so). As D/d increases beyond 2, the packing is usually random (but not always so, as will be shown below for the case $D/d = 2.578$).

Heat transfer: empirical results

As early as 1931, Colburn [5] found that the heat transfer rate for forced convection to air in a packed tube is about eight times higher than that of an unpacked tube. Since then several investigators, including Leva [6], Verschoor and Schuit [7], Plautz and Jhonstone [8], and Quinton and Storrow [9] have published empirical correlation equations for the average heat transfer coefficient for air flow in packed tubes. These correlations exhibit discrepancies as large as 100% from one study to the next. Li and Finlayson [10] suggested that the discrepancies can be attributed to the dependence of the heat transfer coefficient on the length of the packed bed. Dixon and Cresswell [11] speculated that the discrepancies are due to the failure to recognize the influence of additional parameters, such as the ratio of particle to tube diameter, the ratio of fluid to particle thermal conductivity and the fluid Prandtl number. None of these equations accounts for the important parameter called dispersion.

The phenomenon called dispersion can be described qualitatively by comparing the one-dimensional laminar flow of a fluid through a region of space in the presence of, and in the absence of, a porous matrix. In the absence of a porous matrix, the paths of all fluid particles are straight, parallel lines; whereas in the presence of a porous matrix, each fluid particle follows a tortuous path through the interstices of the porous medium. The trajectory of each fluid particle in a porous medium is a random process, the result of which is an overall transverse migration, or 'dispersion', of the particles away from the straight, parallel lines they would have followed in the absence of the porous medium. Dispersion affects the transfer of heat because, in addition to the molecular diffusion of heat, there is mixing due to the aforementioned transverse migration.

Dispersion is a complex phenomenon. A description of it as a second-order tensor is provided in ref. [12] in the presence of heat transfer. The components of this tensor for a given geometry (characterized by d in the present case), are functions of the Reynolds number of the flow, the effective thermal diffusivity, the magnitude of velocity of the fluid through the interstitial spaces in the porous medium, and the pore size of the porous medium (which is, in porous media consisting of spheres of uniform diameter, in turn, a function of the particle diameter d).

Heat transfer: numerical results

Early theoretical analyses of heat transfer in packed tubes were performed by formulating the energy equation corresponding to a simplified model of the actual process. The early models assumed a flat velocity profile which does not take into consideration the nonuniform velocity distribution near the wall due to channeling. In later numerical models [13, 14], the effect of the wall on porosity was taken into consideration. Also, the effect of dispersion on heat transfer was taken into account by introducing a thermal dispersion conductivity as a function of the Peclet number.

The numerical models discussed above utilize equations wherein the fluid velocity, pressure and temperature are averaged within a small local volume. In order for this local volume to represent both global flow variations and local interpore transport, the overall geometry, such as the tube diameter, must be significantly larger than the characteristic length of the particles or pores. In other words, the current models are applicable only for sufficiently high values of D/d. This limitation in the range of applicability of the model results in discrepancies of the order of 25% between the average Nusselt numbers predicted by the numerical model [15] and currently available experimentally determined values for $D/d < 6.7$.

EXPERIMENTAL APPARATUS

The experimental apparatus employed in the present study consisted of a high-precision stainless steel water tunnel which had been previously used to obtain the data reported in ref. [1], and is described therein. This water tunnel is equipped with calibrated orifices that permit measurement of the volume rate of flow through the tunnel. Two new test sections having different inside tube diameters ($D = 0.018542$, 0.015367 m) were built and incorporated into the water tunnel for this investigation. Each of the two test sections consisted of a thin-walled type 304 stainless steel tube 0.5588 m long. An upstream flange contains a hole through which a thermocouple can be inserted to measure the bulk water temperature. Unheated entrance sections of length exceeding $3D$ ensure that the flow is hydrodynamically fully developed† prior to reaching the heated portions of the test sections. A photograph of an installed test section is shown in Fig. 1(a). Detailed drawings appear in ref. [17].

Nearly uniform wall heat flux was achieved in the test sections by passing direct electric currents through the thin stainless steel tube material. Thin coats of insulating varnish were applied over the tubes in order to insulate them electrically from a series of calibrated copper–constantan thermocouples which were attached to the top and bottom of the outer tube walls at 18 locations along the length of the tubes. The test sections were insulated thermally externally with cotton wadding so as to reduce the heat loss from the tubes to the surroundings.

The pressure differences across the test section and across the tunnel orifices were measured with Foxboro differential cells. The weights of the glass spheres loaded into the test sections were measured using an electronic balance having a resolution of ± 0.001 grams. All temperatures were measured using a 40 channel Fluke data acquisition system, whose output was communicated to a computer through a high performance A/D converter which provided a resolution of 1 μV on a 64 mV range. Electrical power was delivered to the test section by means of two Sorensen DCS 20-150B variable power supply units which were connected in parallel to provide a maximum current of 300 A. A water-cooled standard resistor was connected in series with the power supplies. By measuring the voltage drop across the standard resistor, the circuit current was accurately determined.

EXPERIMENTAL PROCEDURE

The glass spheres comprising the matrices of the porous media were tightly packed into the test section to prevent their motion under the action of the flowing water. The water was 'aged' for 24 h prior to use, in order to allow for microscopic air bubbles, which were trapped in the tunnel during the water filling operation, to dissolve; also, the tunnel was always pressurized to approximately 3.5 atmospheres in order to inhibit the formation of air or vapor bubbles.

The experimental procedure was initiated by adjusting the speed of the pump so as to establish a predetermined steady fluid velocity. The power supply was then turned on and adjusted to cause an electric current to flow through the tube wall that raised the tube wall temperature by a small predetermined amount. The inlet bulk water temperature, the 36 measured temperatures of the tube wall and the voltage drop across the standard resistor were recorded at intervals of 5 min. The temperature data were recorded directly into the computer using a Quick Basic program that calculated the difference between the tube wall temperatures recorded at the current time step and at the previous time step for each axial location. When the absolute value of this difference at each axial location was less than 0.01°C over a period of 15 min the system was deemed to have reached a steady state. The steady-state values of the tube wall temperatures were stored in a separate computer file for use in subsequent calculations.

Having recorded the measurements corresponding to one so-called 'data point' as described above, the electrical power supply was then adjusted to create

† The hydrodynamic entry length for packed tubes does not exceed 1 tube diameter [15].

(a)

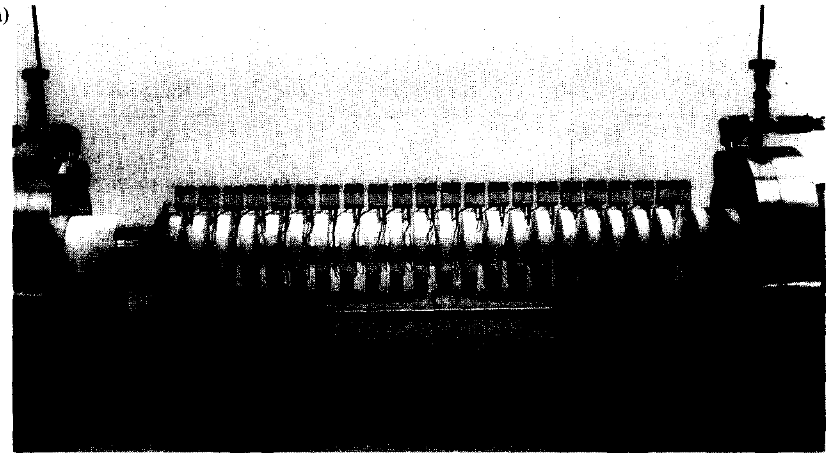

(b)

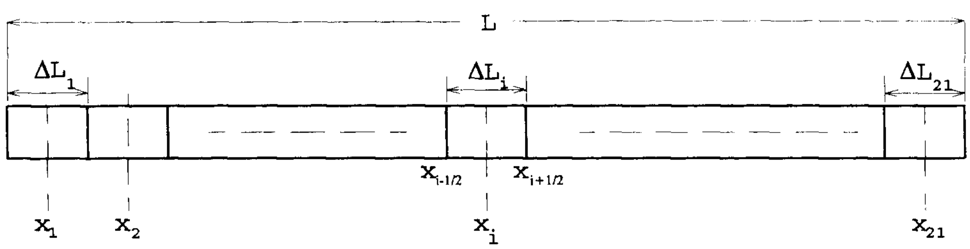

Fig. 1. Test section, (a) photograph of installed test section, (b) subdivision of test section for evaluating the local Nusselt number. Thermocouples were located at stations 1, 3, 5 and 7–21 at top and bottom of tubes.

progressively higher temperature differences between the tube wall and the inlet fluid, thereby providing data for various temperature differences at the predetermined velocity. By varying the pump speed, the flow velocity was altered to obtain information in the Darcy, Forchheimer and the turbulent regimes. The D/d ratio was altered by filling either of the two test sections having different diameters with glass spheres having different diameters. Table 1 shows the ranges of the relevant parameters for the data collected in this investigation.

DATA ANALYSIS AND RESULTS

Calculation of the local Nusselt number

In order to evaluate the local heat transfer coefficient, the test section of length L was divided into 21 parts designated by ΔL_1, $\Delta L_2, \ldots, \Delta L_i, \ldots, \Delta L_{21}$ with centerline locations designated by X_i as indicated in Fig. 1(b). The inner surface temperatures of the heated tube, which are needed to calculate the heat transfer coefficient, were obtained from the measured outer surface temperature readings by solving the controlling differential equation for conduction in a radial system with uniform heat generation. The differences between the inside and outside temperatures were insignificant.

The heat flux for each ΔL_i was calculated from the wattage dissipated in each ΔL_i. The local resistance† of the tube wall corresponding to its (measured) local temperature was used in this calculation. The energy balance equating the total rate of heat input to the ith section between the positions $X_{i-1/2}$ and $X_{i+1/2}$ to the rate of heat absorbed by the water stream in this section is given by

$$q_i = \dot{m}c_p(T_{i+1/2} - T_{i-1/2}), \tag{16}$$

where $\dot{m}$ is the mass flow rate of water, c_p is the specific heat of water, $T_{i-1/2}$ and $T_{i+1/2}$ are the mean temperatures of the water at the inlet and exit of the ith section, and q_i is the rate of convective heat transfer in the ith section.

The quantity q_i equals the difference between the rate of heat generation and the rate of external heat loss at the ith section and is given by

$$q_i = I^2 R_i(\Delta L_i) - (q_l)'_i(\Delta L_i), \tag{17}$$

where I is the electric current flowing through the test cylinder wall, R_i is the resistance of test cylinder per unit length at the mean cylinder wall temperature $(T_w)_i$, and $(q_l)'_i$ is the rate of external heat loss per unit

† The local resistance was obtained from an equation relating resistance to temperature for type 304 stainless steel. The maximum change in the tube wall resistance due to temperature variation, and therefore in heat flux, in any test was 4.9%.

Table 1. Ranges of experimental parameters

Test/Series*	No. of data (N)	D ($\mathrm{m} \times 10^3$)	d ($\mathrm{m} \times 10^3$)	D/d	Range of Re_d	Range of Pr (with k_λ)
A1	38	18.542	1.242	14.929	0.73–98.1	2.6–4.9
A2	52	18.542	2.010	9.229	1.33–313	2.6–4.8
A3	65	18.542	2.988	6.206	9.19–702	3.7–4.9
A4	36	18.542	3.996	4.641	19.7–650	3.8–5.0
A5	45	18.542	4.992	3.714	24.6–785	4.1–4.9
A6	75	18.542	5.962	3.110	41.4–992	3.8–5.0
A13	54	18.542	13.467	1.377	74.1–2168	3.9–5.3
B3	37	15.367	2.988	5.143	9.1–594	2.5–4.9
B4	40	15.367	3.996	3.846	38.5–981	2.6–4.9
B5	77	15.367	4.992	3.078	48.4–1134	2.5–4.9
B6	48	15.367	5.962	2.578	19.4–1542	2.6–5.0
B13	51	15.367	13.467	1.141	108–3148	2.6–5.2

*In this column, A represents the 18.542 mm tube and B represents the 15.367 mm tube. The numbers following the letters represent the nominal diameters in millimeters of the glass spheres.

length of the tube†. The value of $(T_w)_i$ was taken to be the average value of the inner surface temperatures at the top and bottom of the tube.

Starting with the measured bulk temperature of water at the inlet to the first section, equation (16) was applied successively to each of the 18 sections ($i = 1, 2, \ldots, 18$) of the test cylinder to obtain the bulk temperature of water at the exit of each section. The average value of the heat transfer coefficient for the ith section, h_i, was then calculated using the relation

$$q_i = h_i(\pi D)(\Delta L_i)[(T_w)_i - T_i], \qquad (18)$$

where $T_i = [T_{i+1/2} + T_{i-1/2}]/2$ and D is the inside diameter of the tube.

Using these values of h_i, the local Nusselt number for each section was then evaluated from $Nu_i = h_i D/k_\lambda$, where k_λ is the effective thermal conductivity given by the following equation [18]:

$$k_\lambda = k_f \lambda^{-n}, \qquad (19)$$

where $\lambda = k_f/k_s$ and $n = 0.280 - 0.757 \log_{10}\varepsilon + 0.057 \log_{10}\lambda$.

Identification and elimination of the mixed convection regime

Since the present study is concerned with forced convection in packed tubes, it was necessary to identify and eliminate those experimental data in which natural convection was not negligible. In the mixed convection regime, wherein both natural and forced convection effects are important, the fluid inside the tube is thermally stratified due to natural convection effects, causing circumferential variation of the tube wall temperature. The greater the circumferential variation in temperature, the greater is the importance of natural convection relative to forced convection. The quantity $(T_{w,top} - T_{w,bot})$, where $T_{w,top}$ and $T_{w,bot}$ are the measured temperatures of the top and bottom of the horizontal tube wall at a given axial station, is the maximum circumferential variation in the tube wall temperature and is, therefore, the most sensitive measurable index to the relative importance of natural to forced convection.

The following arbitrary quantitative criterion was adopted in the present study to identify those data for which natural convection effects are considered to be negligible compared to forced convection effects. Forced convection was considered to be the predominant mode of heat transfer for those experiments in which the maximum measured value of $(T_{w,top} - T_{w,bot})$ was less than 2% of the maximum measured value of $(T_{w,top} - T_0)$, where T_0 is the inlet water temperature; symbolically,

$$\frac{(T_{w,top} - T_{w,bot})_{max}}{(T_{w,top} - T_0)_{max}} \times 100 < 2\%. \qquad (20)$$

Experiments that satisfied the above criterion provided the set of data upon which the correlations determined in this study were based. The data obtained in experiments that violate this (conservative) criterion were assumed to represent mixed convection data and were disregarded. It is to be understood that all data discussed hereinafter come from experiments that satisfy the forced convection criterion.

Identification of the thermally fully developed region

In order to identify the thermally fully developed region for the present problem of flow through a packed tube with uniform wall heat flux, it is useful to consider the analogous situation for a tube with uniform wall heat flux with no packing. For the case of uniform wall heat flux in an unpacked tube, it is well known that the bulk temperature T_b rises linearly

† The rate of external heat loss from the tube was determined by experiments with empty tubes described in ref. [17].

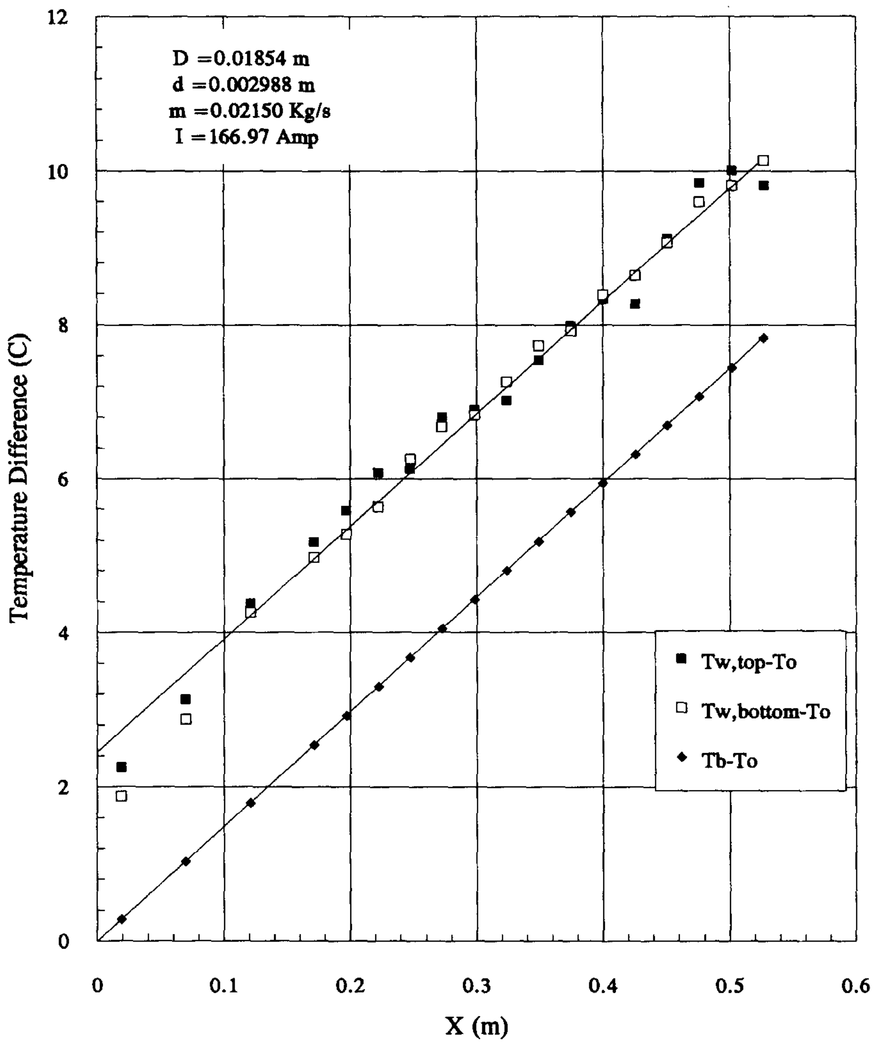

Fig. 2. Axial variation of wall and fluid temperatures for test A3.

downstream and that in the fully developed thermal region, the wall temperature T_w also rises linearly and at the same rate as T_b. Similarly, for the present problem of internal flow through a packed tube with uniform wall heat flux, the thermally fully developed region can be identified by observing how far downstream the measured values of T_w and T_b plot as straight lines having the same slopes.

Figure 2 shows a typical plot of the axial variation of measured values of T_w and calculated values of T_b obtained in the present study. The difference $(T_b - T_0)$ is everywhere very nearly proportional to the downstream distance X; thus

$$T_b - T_0 = aX, \tag{21}$$

where the value of slope a can be obtained by linear regression. For the thermally fully developed region, $(T_w - T_0)$ may be expressed as follows:

$$T_w - T_0 = aX + b, \tag{22}$$

where a is as determined by equation (21) and b is an intercept. For all forced convection data obtained in this study, it was observed that $(T_w - T_0)$ was nearly constant for $X/D \geqslant 8$. Thus, the value of b was obtained by linear regression using the measured values of $(T_w - T_0)$ for $X/D \geqslant 8$.

Subtracting equation (21) from equation (22) yields:

$$T_w - T_b = b. \tag{23}$$

The value of $(T_w - T_b)$ per equation (23) together with the known experimental value of q'' permitted the evaluation of the constant heat transfer coefficient ($h = q''/b$) for the thermally fully developed region.

Formulation of a correlation hypothesis for Nu

An empirical correlation of experimental data is usually developed by adopting an appropriate hypothesis which consists of a mathematical equation containing arbitrary constants, and then determining the numerical values of the constants by fitting the equation to the experimental data. The method followed here to determine a correlation hypothesis was to adopt mathematical forms based on previous experience, and then modify these forms based upon physical reasoning not heretofore applied.

In order to correlate the experimental data assembled in this study, it was assumed that the internal flow through a heated packed tube can be conceptually decomposed into two components, a 'coarse' component and a 'fine' component. The coarse component is a flow that has a velocity at every point in the field. The velocity of the coarse flow (which is a fiction because it has a value at every point in a porous medium, even though much of the volume comprising a porous medium consists of solid material) is the volume-averaged velocity that is defined conventionally in many studies of flow through porous media (e.g. the 'superficial' velocity in Darcy flow). The fine component of flow refers to a superimposed meandering flow through the interstitial spaces between the particles in a porous medium and gives rise to the phenomenon called dispersion.

It was further assumed that the Nusselt number is expressible as the product of three functions, f_1, f_2 and f_3, where f_1 represents the influence of the 'coarse' component of flow on the heat transfer, f_2 represents the influence of the 'fine' component of flow, and f_3 represents the interaction between the coarse and fine flow. This assumption can be expressed symbolically as follows:

$$Nu = Cf_1f_2f_3. \tag{24}$$

The function f_1 was taken to be the following generalized product form:

$$f_1(Re_D^m, Pr^\Psi) = C_1(Re_D^m)(Pr^\Psi), \tag{25}$$

where C_1, m and Ψ are constants; and the function f_2 was taken to be

$$f_2 = C_2(Pr^\omega)g(Di), \tag{26}$$

where C_2 and ω are constants and Di is a dimensionless measure of dispersion. The measure of the effect of dispersion adopted here is based on the hypothesis developed by Fand *et al.* [16] in connection with their study of forced convection heat transfer from cylinders embedded in porous media. The reasoning that led to the development of a suitable measure of dispersion is discussed in the following.

The measure of dispersion, Di, was known to be a function of Re_d; however, because of the complexity of the process, it was anticipated that the determination of an appropriate measure of dispersion that is expressible directly as a function of Re_d and also possesses certain other requisite properties (to be described presently) would be difficult to achieve. It was surmised that a suitable measure of dispersion could be more readily determined in terms of the pressure gradient, via the *dimensionless friction factor* f_w, which is, in turn, a known function of the particle Reynolds number Re_d per equations (8)–(10). However, f_w, by itself, does not represent a suitable choice for Di for the following reason: if one considers a given heated tube (given D) and supposes that the tube is successively packed with a series of porous media that are saturated by the same fluid and are subjected to the same flow velocity (identical Re_D), but have diminishing particle sizes (d and $Re_d \to 0$), then, for such a series of experiments one would expect the Nusselt number to approach a finite limit. But f_w increases beyond all bounds as $Re_d \to 0$, and hence f_w is not a suitable measure of dispersion in the function g. However, the quantity f_wRe_w is suitable from this point of view, because this quantity remains finite as $Re_d \to 0$. Hence, the measure of dispersion adopted here is

$$Di = f_wRe_w. \tag{27}$$

The next step in formulating the hypothesis was to determine a form of the function $f_3(D/d)$† that will account for the interaction between the fine and coarse flows. It can be readily seen that a simple function such as $(D/d)^n$ is not suitable because $(D/d)^n$ exceeds all bounds as $d \to 0$. A power function of arctan $(D/d)^n$ was adopted here because arctan $(D/d)^n$ monotonically approaches a finite upper bound ($\pi/2$) as $d \to 0$. The aforestated reasoning led to the adoption of the following form for f_3:

$$f_3 = C_3[\arctan(D/d)^n]^r, \tag{28}$$

where C_3, n and r are constants.

Taken together, the foregoing reasoning and assumptions lead to the following correlation hypothesis for the Nusselt number:

$$Nu = C\,Re_D^m(Pr^p)(f_wRe_w)^q[\arctan(D/d)^n]^r, \tag{29}$$

where $C = C_1C_2C_3$ and $p = \psi + \omega$.

Development and evaluation of correlation equations

The nondimensional parameters Re_D, Pr, f_wRe_w and Nu in equation (29) were evaluated using thermophysical properties at the mean bulk temperature of the fluid, $T_{b,m} = (T_{b,i} + T_{b,o})/2$, where $T_{b,i}$ and $T_{b,o}$ are the bulk temperatures of the fluid at the inlet and outlet of the test section, respectively. The values of the constants in equation (29) were obtained by an optimization procedure described in ref. [17].

It may be noted from a comparison of equations (11) and (12) that the five flow parameters (k, A_w, B_w, A'_w and B'_w) that characterize the fluid flow in packed tubes behave differently below $D/d = 1.40$ (where they are monotonically decreasing with increasing D/d) from what they do above $D/d = 1.40$ (where they are monotonically increasing with increasing D/d). Since

† Note that f_3 $(Re_D/Re_d) = f_3(D/d)$ if properties for the coarse and fine flows are assumed equal.

Table 2. Optimum numerical values of constants in equation (29)

Regime	m	n	C	p	q	r
For $3 < D/d < 15$; $X/D \geqslant 8$						
Darcy	0.5	0.5	0.5016	0.4067	0.1912	0.9117
Forchheimer	0.5	0.5	0.2016	0.3671	0.3329	2.1819
Turbulent	0.5	0.5	0.1853	0.3308	0.3788	2.2416
For $D/d = 1.4, 1.1$; $X/D \geqslant 8$*						
Turbulent	0.25	1	0.2146	0.4054	0.5260	−0.6511

*Adequate data were available only in the turbulent regime.

the test series A13 and B13 have D/d values less than 1.40, and hence their flow characteristics differ from the others, it was anticipated that the correlation constants for these two test series would differ from the others, and so were treated as a separate group.

An interesting anomaly was observed for the test series with D/d of 2.578. It was found that the spherical particles arranged themselves in portions of the tube in a regular helical pattern leaving a clear hole through the center of the helix. The tube was packed a number of times and it was found that the depth of the holes through its center varied each time. It was concluded that the packing method did not result in random or repeatable packings for $D/d = 2.578$ and hence, the results of this test series were excluded from further consideration.

The optimum numerical values of the constants in equation (29) are listed in Table 2. Figs 3–5 are plots that show the performance of equation (29) in the Darcy, Forchheimer and turbulent regimes for $D/d > 1.40$. In these figures, points that fall on the 'main diagonal' line through the origin with a slope equal to one indicate perfect agreement between Nu_{cal} and Nu_{exp}. Sample sets of data, selected at random from each relevant data subset, are plotted in these figures because these sample data are sufficient for the present purpose and are not so numerous as to render their graphical representations confusing.

Table 3 lists the errors incurred by equation (29) for fully developed flow ($X/D \geqslant 8$) for the nine tests with random packing ($3 < D/d < 15$) and for the two tests with deterministic packing ($D/d = 1.4, 1.1$). The magnitude of the mean error is less than 3.6% in all cases; and the mean deviation is between 6 and 10% for all tests except for $D/d = 1.1$, for which it is 23%. Further, the maximum deviation is nearly constant (between 15 and 18%) for the random packings and rises to 37% for $D/d = 1.4$ and to 88% for $D/d = 1.1$. An explanation for this pattern of rising maximum deviations (and associated mean deviations) follows.

Table 3. Errors incurred by equation (29)

Regime	$E_{\mathrm{m}}(\%)$	$E_{\mathrm{md}}(\%)$	$E_{\mathrm{maxd}}(\%)$
For $3 < D/d < 15$ and $X/D \geqslant 8$			
Darcy	−0.44	6.25	15.7
Forchheimer	−2.55	7.72	17.9
Turbulent	−1.82	7.75	18.2
For $D/d = 1.4, 1.1$; $X/D \geqslant 8$			
Turbulent(1.4)	2.85	9.61	36.5
Turbulent(1.1)	−3.57	22.4	87.8

The explanation is based upon the physical fact, which becomes obvious if one considers the pattern of fluid flow, that the local heat transfer coefficient in a tube packed with spheres must be a function that is periodic in both the axial and circumferential directions; further, both the wavelength and amplitude of this function must increase with a decrease in D/d. Now, the surface temperature measurements made in the present study, and therefore the Nusselt numbers calculated therefrom, constitute finite (yet adequate) random samples taken from infinite sets. The maximum (and mean) deviations listed in Table 3 are consistent with the physical fact that the periodic function, which represents the local Nusselt number, is characterized by increasingly larger amplitudes as D/d approaches unity.

APPLICATION TO HEAT TRANSFER ENHANCEMENT

This section focuses on the enhancement of heat transfer achievable by packing tubes with glass spheres and the associated friction power requirements. The heat transfer enhancement achieved using packed tubes will be compared to the use of typical twisted tape inserts and longitudinal integral fins under the constraint of constant pumping power.

Heat transfer and flow-friction characteristics in packed tubes

Kays and London [19] have developed a consistent treatment of basic heat transfer and flow-friction data for compact heat exchanger surfaces, so as to avoid the confusion often encountered with a large number

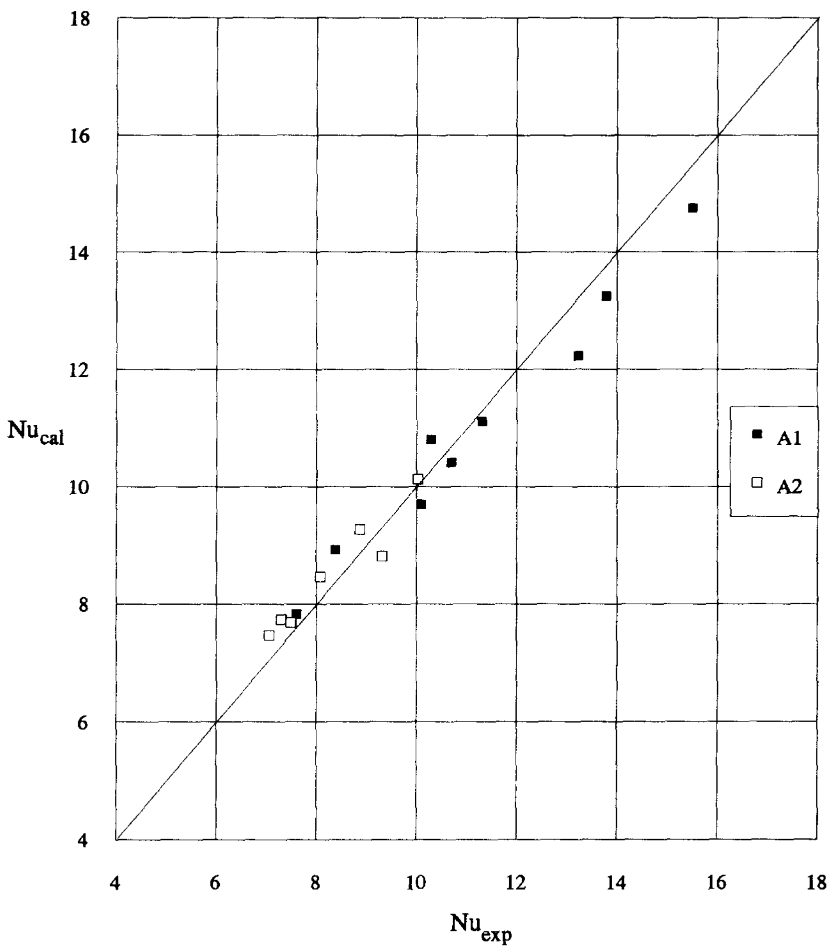

Fig. 3. Graph of equation (29) for Darcy flow.

of arbitrarily defined parameters. Following their method of treatment, the basic heat transfer and flow-friction performance data for packed tubes are presented in the following forms:

$$St\,Pr^{2/3} = \phi_1(Re_D), \tag{30}$$

$$f = \phi_2(Re_D), \tag{31}$$

where $St = Nu/(Re_D Pr)$ is the Stanton number, $f = P'D\varepsilon^3/2\rho u^2$ is the flow-friction factor, ϕ_1 and ϕ_2 are functions of Re_D. In this context, the fluid thermal conductivity, k_f, is used in the evaluation of Pr and St.

The heat transfer and flow-friction performance curves for packed tubes per equations (30) and (31) are presented in Figs 6 and 7 for the turbulent regime. The correlation equation (29) developed in this study is used to generate these plots. Similar plots can be obtained for Darcy and Forchheimer regimes and are presented in ref. [17]. Figures 6 and 7 show the variation of $StPr^{2/3}$ and f as functions of Re_D and D/d. It can be observed that the rate of heat transfer and the friction factor increase with increasing D/d for a given Re_D.

Evaluation of heat transfer enhancement

An evaluation of the heat transfer enhancement achieved by packing a tube with spheres may be made by comparing the heat transfer characteristics of the packed tube with that of an unpacked smooth tube (relevant parameters designated by subscript s). The Nusselt number, Nu_{ls}, and the friction factor, f_{ls}, for fully developed laminar flow in smooth tubes with uniform wall heat flux are given by [20]

$$Nu_{ls} = 4.364; \quad f_{ls} = 16/Re_s. \tag{32}$$

For fully developed turbulent flow in smooth tubes with uniform wall heat flux, the Nusselt number is given by [20]

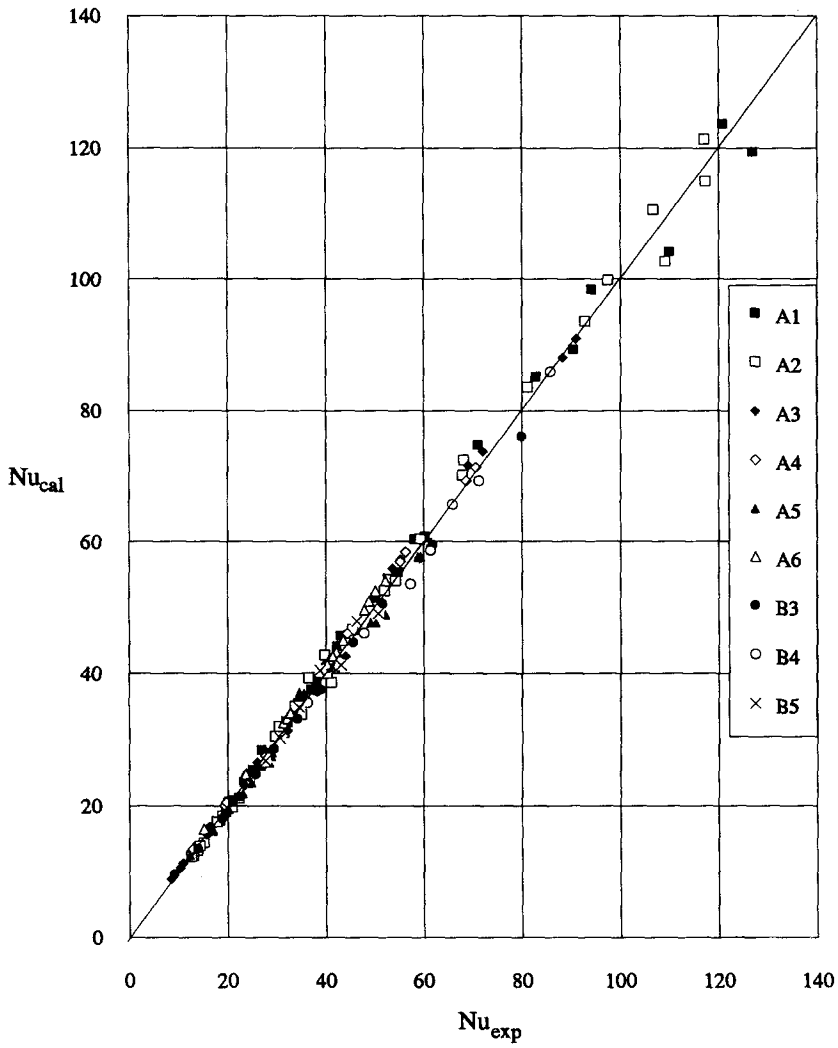

Fig. 4. Graph of equation (29) for Forchheimer flow.

$$Nu_{ts} = \frac{(f_{ts}/2)(Re_s - 1000)Pr}{1 + 12.7(f_{ts}/2)^{0.5}(Pr^{2/3} - 1)}, \tag{33}$$

where the friction factor f_{ts} is given by

$$f_{ts} = [1.58\ln(Re_s) - 3.28]^{-2}. \tag{34}$$

Using equations (29), (32) and (33) the enhancement ratio (ratio of Nusselt number for a packed tube to that of an unpacked smooth tube) can be calculated for laminar and turbulent flow. Figures 8 and 9 show the enhancement ratios of packed tubes with D/d of 3.110 and 9.229 under the constraint of equal pumping power for laminar and turbulent flows, respectively. These figures show that the enhancement ratios achieved with $D/d = 3.110$ is about 25% more than that achieved with $D/d = 9.229$ for laminar flow and 75% more for turbulent flow. Also, the enhancement achieved using packed tubes with D/d of 3.110 is two to seven times more than that of unpacked tubes for laminar flow and two to two and a half times more for turbulent flow.

In order to compare the heat transfer enhancement achieved using packed tubes with that of an internally finned tube (FT) and a tube with twisted tape inserts (TT), the following typical geometric parameters for the internally finned tube and the tube with twisted tape inserts are used:

FT	TT
Number of fins = 8	Tape thickness = $0.045D$
Fin height = $0.2D$	Twist ratio $y = H/D = 2.5$*
Fin thickness = $0.04D$	*H = axial distance for 180° twist

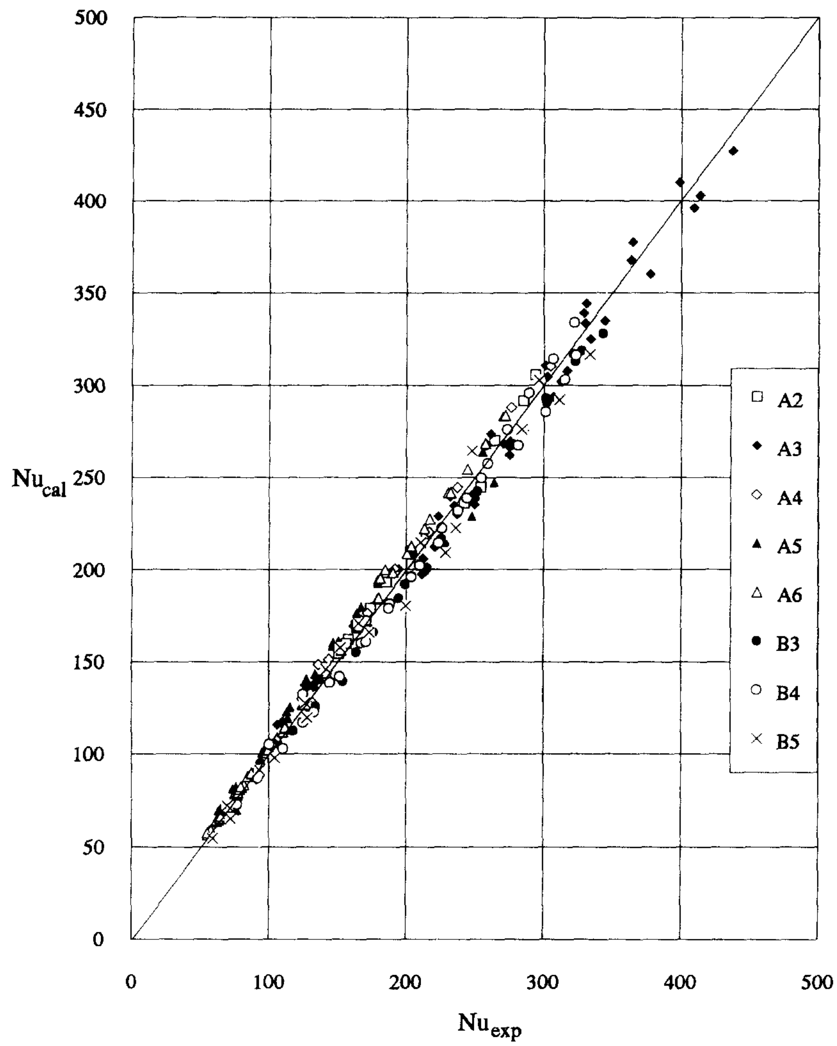

Fig. 5. Graph of equation (29) for turbulent flow.

Figure 8 shows the enhancement ratio obtained with equal pumping power for Test Series A2 ($D/d = 9.229$), Test Series A6 ($D/d = 3.110$), FT and TT for laminar flow. The details of the calculations are presented in ref. [17]. It can be seen that the enhancement ratios of the packed tubes are substantially greater than FT for $Re_s > 300$. The enhancement ratios of the packed tube with D/d of 3.110 and TT are nearly equal, but TT performs better for $D/d > 3.110$. Figure 9 shows the enhancement ratio obtained with equal pumping power for two different packings, FT and TT for turbulent flow. It can be seen that the packings do not provide any substantial advantage over FT and TT.

From the above observations, the following conclusions can be drawn regarding the enhancement of heat transfer achieved using packed tubes *for equal pumping power*:

(1) A packed tube having a lower D/d provides more heat transfer enhancement than one with a higher D/d for $D/d > 1.40$

(2) The heat transfer enhancement achieved using packed tubes can be two to seven times more than that of unpacked tubes for laminar flow and two to two and a half times more for turbulent flow.

(3) For laminar flow, the enhancement ratio of packed tubes can be two to four times more than that of finned tubes and nearly the same as that of tubes with twisted tape inserts.

(4) For turbulent flow, the enhancement ratio of

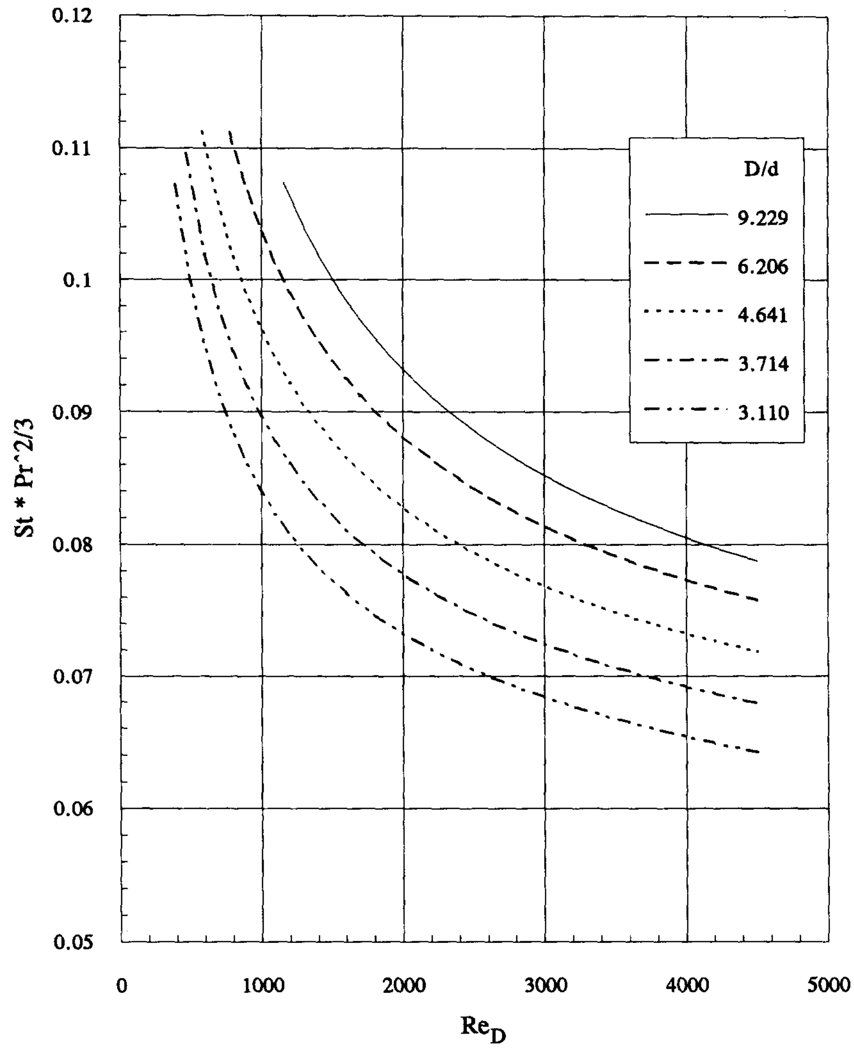

Fig. 6. Heat transfer characteristics in the turbulent regime per equation (30).

packed tubes is nearly the same as that of finned tubes and tubes with twisted tape inserts.

CONCLUSION

It has been demonstrated that equation (29), with appropriate constants for Darcy, Forchheimer and turbulent flow, represents the mean values of Nu obtained in this study for $D/d > 1.40$ and $X/D > 8$ (where the flow is thermally fully developed) with a degree of accuracy that is deemed acceptable for design purposes. This empirical correlation equation is based upon a hypothesis that regards the flow in a porous medium to be the superposition of a 'fine' component upon a 'coarse' component, and takes into account the effect of the wall and the influence of dispersion upon heat transfer for the geometry considered herein. It has been found that the dimensionless measure of dispersion, Di, utilized in a previous study [16] of (external) forced convection heat transfer from isothermal cylinders embedded in porous media is applicable to the present geometry as well.

The results of this study show that for equal pumping power the method of packing tubes with spheres can provide heat transfer enhancement two to seven times that of unpacked tubes for laminar flow and two to two and a half times for turbulent flow. For laminar flow with equal pumping power, packed tubes can provide greater heat transfer enhancement than finned tubes and can equal the enhancement achievable with twisted tape inserts. For turbulent flow with

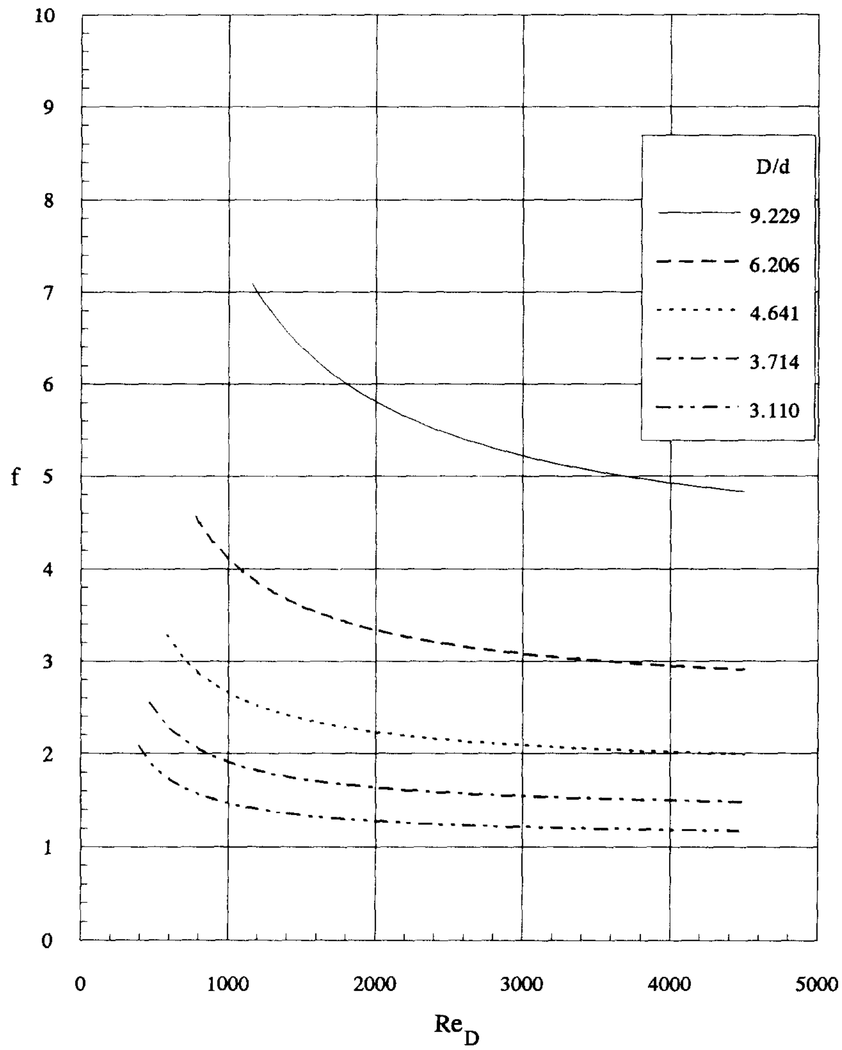

Fig. 7. Flow-friction characteristics in the turbulent regime per equation (31).

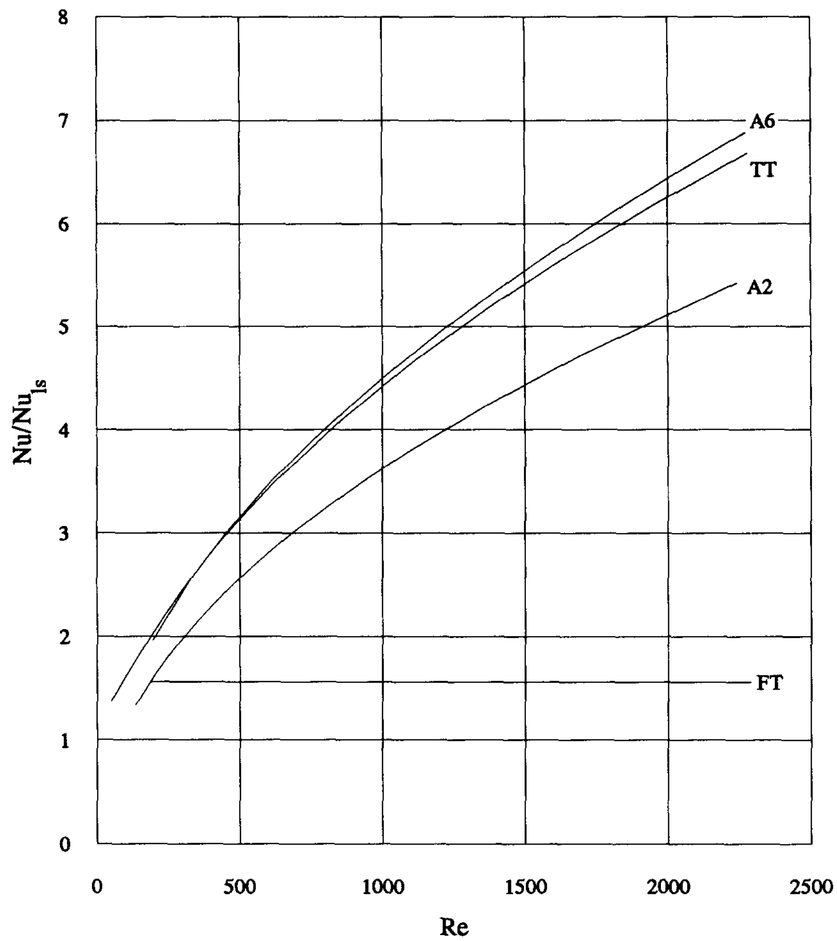

Fig. 8. Enhancement ratio for laminar (Darcy and Forchheimer) flow with equal pumping power.

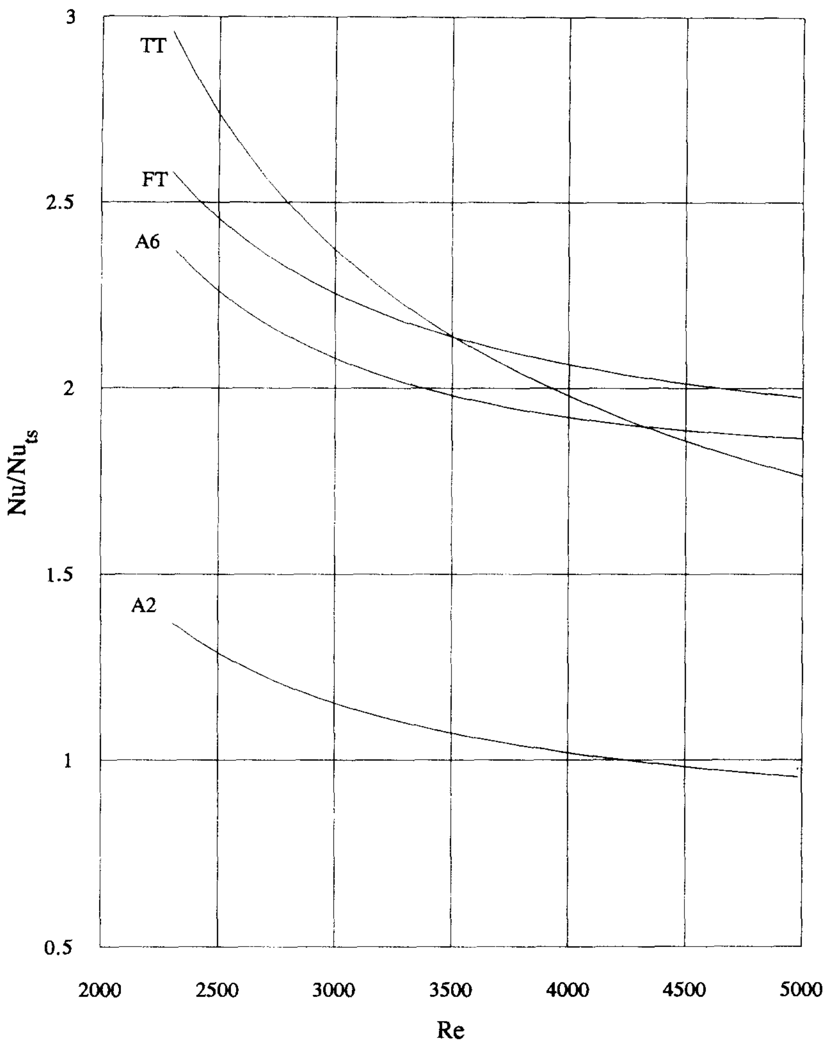

Fig. 9. Enhancement ratio for turbulent flow with equal pumping power.

equal pumping power, packed tubes can equal the heat transfer enhancement achievable with finned tubes and tubes with twisted tape inserts.

REFERENCES

1. R. M. Fand, B. Y. K. Kim, A. C. C. Lam and R. T. Phan, Resistance to the flow of fluids through simple and complex porous media whose matrices are composed of randomly packed spheres, *ASME J. Fluids Engng* **109**, 268–273 (1987).
2. R. M. Fand and R. Thinakaran, The influence of the wall on flow through pipes packed with spheres, *ASME J. Fluids Engng* **112**, 84–88 (1990).
3. R. M. Fand, M. Sundaram and M. Varahasamy, Incompressible fluid flow through pipes packed with spheres at low dimension ratios, *ASME J. Fluids Engng* **115**, 169–172 (1993).
4. W. Reichelt, Zur berechnung des druckverlustes einphasig durchstroemter kuger-ung zylinder-schuettungen (calculation of pressure drop in spherical and cylindrical packings for single phase flow), *Chem.-Ing. Tech.* **44**, 1068–1071 (1972).
5. A. P. Colburn, Heat transfer and pressure drop in empty baffled and packed tubes, *Ind. Engng Chem.* **23**, 910–923 (1931).
6. M. Leva and M. Grummer, Heat transfer to gases through packed tubes: effect of particle characteristics, *Ind. Engng Chem.* **40**, 415–419 (1948).
7. H. Verschoor and G. C. A. Schuit, Heat transfer to fluids flowing through a bed of granular solids, *Appl. Sci.* **42**, 97–119 (1952).
8. D. A. Plautz and H. F. Jhonstone, Heat and mass transfer in packed beds, *Am. Inst. Chem. Engrs J.* **1**, 193–199 (1955).
9. J. H. Quinton and J. A. Storrow, heat transfer to air flowing through packed tubes, *Chem. Engng Sci.* **5**, 245–257 (1956).
10. C. H. Li and B. A. Finlayson, Heat transfer in packed beds—a reevaluation, *Chem. Engng Sci.* **32**, 1055–1066 (1977).
11. A. G. Dixon and D. L. Cresswell, Theoretical prediction of effective heat transfer parameters in packed beds, *Am. Inst. Chem. Engrs J.* **25**, 663–675 (1979).
12. D. A. Nield and A. Bejan, *Convection in Porous Media*. Springer, New York (1992).
13. P. Cheng and D. Vortmeyer, Transverse thermal dispersion and wall channeling in a packed bed with forced convective flow, *Chem. Engng Sci.* **43**, 2523–2532 (1988).
14. P. Cheng, Wall effects on fluid flow and heat transfer in porous media, *Proceedings of the Second ASME/JSME Thermal Engineering Conference*, Vol. 2, pp. 297–303 (1987).

15. A. Chowdhury, A numerical study of mixed and forced convection in a vertical packed tube and a packed channel, Ph.D dissertation in Mechanical Engineering, University of Hawaii, supervised by P. Cheng (1992).
16. R. M. Fand, M. Varahasamy and L. S. Greer, Empirical correlation equations for heat transfer by forced convection from cylinders embedded in porous media that account for the wall effect and dispersion, *Int. J. Heat Mass Transfer* **36,** 4407–4418 (1993).
17. M. Varahasamy, Heat transfer by forced convection in pipes packed with porous media whose matrices are composed of spheres, Ph.D dissertation in Mechanical Engineering, University of Hawaii, supervised by R. M. Fand (1995).
18. V. Prasad, N. Kladias, A. Bandyopadhaya and Q. Tian, Evaluation of correlations for stagnant thermal conductivity of liquid-saturated porous beds of spheres, *Int. J. Heat Mass Transfer* **32,** 1793–1796 (1989).
19. W. M. Kays and A. L. London, *Compact Heat Exchangers*. McGraw-Hill, New York (1984).
20. F. P. Incropera and D. P. DeWitt, *Introduction to Heat Transfer*. Wiley, New York (1990).